Molecular orbital *ab initio* and density functional theoretical study on reaction between PH_2 and NO

HU Zhengfa (胡正发), WANG Zhenya (王振亚), LI Haiyang (李海洋) & ZHOU Shikang (周士康)

Laboratory of Environment Spectroscopy, Anhui Institute of Optics and Fine Mechanics, Chinese Academy of Sciences, Hefei 230031, China
Correspondence should be addressed to Zhou Shikang (email: skzhou@aiofm.ac.cn)

Received December 15, 2001

Abstract The theoretical study of reaction between PH_2 and NO on the ground state potential energy surface is reported by using molecular orbital *ab initio* calculation and density function theory (DFT). Equilibrium structural parameters, harmonic vibrational frequencies, total energies and zero point energies of all species during reaction are computed by HF, MP2 (full) and B3LYP theory levels with the medium basis set 6-31G*. Theoretical results indicate that intermediate IM1(H_2PNO) is firstly formed by overcoming a small energy barrier TS1, and then two four-membered ring transient states TS2 and TS5, with energy barriers 103.3 and 102.6 kJ/mol respectively, then H-migration and isomerization are completed and the products PN and H_2O are formed. The reaction is exothermic one with –189.6 kJ/mol released.

Keywords: quantum chemistry *ab initio*, B3LYP theory level, reaction potential surface, PH_2 radical.

PH_x plays an important role in biochemistry, photochemistry of interstellar atmosphere, combustion and environmental chemistry[1—6]. PH_3 is the key component in the atmosphere of Jupiter and Saturn[7—9]. It also participates in chemical vapor deposition processes for the manufacturing of semi-conductors[10,11]. In the research of their properties, Pierini and Duca[12] reported the proton affinities of phosphinidene by AM1 and PM3 methods. Jursic[13] calculated ionization potentials (IP) and electron affinities of PH_x, PHF, PF_x with CBS, MP2 and DFT theory. Three low-lying electronic states have been investigated systematically by Woodcock[14] using *ab initio* electronic structure theory. And Goto and Saito[15] observed the lowest rational spectral lines of PH radical in its ground vibronic state by submillimeter-wave spectra. With respect to the reaction, Mercier et al.[16] have studied the reaction mechanism of alkene addition of complex (R-P-W$(CO)_5$) and found their electrophilic carbene-like nature. Nahas and Hirao[17] performed theoretical study on complexation of Li^+ and Cu^+ with PH_2, and concluded that the reaction was dominated by charge transfer (CT) from the H atoms to metal center through P atom.

NO_x has been recognized as pollutants in atmosphere and exerts great influence on reduction and depletion of ozone in the stratosphere[18,19]. But the reaction, PH_2+NO, thitherto, has been less studied. For PH_2, the data available in literature concern essentially the photophysical processes undergone by the excited $\tilde{A}\,^2A_1$ and ground $\tilde{X}\,^2B_1$ electronic states in collision with other

molecules. Limited results were obtained in experiment[20]. Only two experiments have been reported dealing with the recombination reaction PH_2+PH_2, and the reactions with NO and O_2[3,20]. Very recently Xuan et al.[1] determined the rate constants of the reactions PH_2 ($\tilde{X}^2B_1$; v'' = 0,1)+NO, which were $(5.47 \pm 0.54)\times 10^{-14}$ (v'' = 0) and $(6.68 \pm 1.57)\times 10^{-12}$ cm^{-3} •mol^{-1} •s^{-1} (v'' = 1) respectively by LIF experiment at room temperature, however the reaction channel was estimated. To our best knowledge, accurate investigation of reaction channels and products of PH_2+NO has not been reported both experimentally and theoretically.

In the present paper, the reaction PH_2+NO is studied theoretically by using *ab initio* molecular orbital (MO) and density function theory (DFT) on a double potential energy surface. The reaction channel is worked out, and equilibrium geometries, harmonic frequencies and total energies of each stationary point species through reaction channel are listed. The computation result was in agreement with Xuan's[1] estimation for reaction mechanism and has potential meaning to environmental protection and nitrogen cycle[21] in atmosphere.

1 Methodology

ab initio molecular orbital (MO) and density function theory (DFT) calculations have been performed with Gaussian98 program package[22]. The optimized geometries and harmonic frequencies of all species were obtained at the HF, MP2 (full) and B3LYP with the same basis set 6-31G*, and the frequencies for all required structures were evaluated at B3LYP/6-31G* level to ascertain the nature of stationary points, meanwhile the zero point energies (ZPE) were obtained based on frequency computation. Total energies of all species were calculated at MP2(full)/6-31G*, G3 and B3LYP/6-31G*[23], however that of transition states was got at MP2(full)/6-31G* and B3LYP/6-31G* level. Moreover, the intrinsic reaction coordinate (IRC) method at the B3LYP/6-31G* level was also used to further analyze the characteristics of the channels.

2 Results and discussion

2.1 Optimized geometry

Fig. 1 shows the schematic diagrams of all species with the optimized geometry parameters, which were obtained at B3LYP/6-31G* level and listed in table 1. Let's take PH_2 as an example. Its experimental equilibrium bond length r_e equals 1.418 Angstrom and the bond angle is $\angle$HPH = 91.7°[3], where MP2 result (1.4186 Å) is close to r_e; on the other hand, the bond angle from B3LYP (91.6°) is much better than at two other levels. For NO, the bond length 1.1587 Angstrom of B3LYP is closest to the experimental value 1.1508 Angstrom[24] in the three methods. Furthermore, the experimental results of H_2O and PN molecules support the result with B3LYP theory. Table 2 lists optimized geometry parameters of all transition states. From the data shown in fig.1 and tables 1 and 2, the reaction occurred when N atom in NO collided with P atom of PH_2 along the direction of molecular axis to form the addition product IM1. The intermediate species

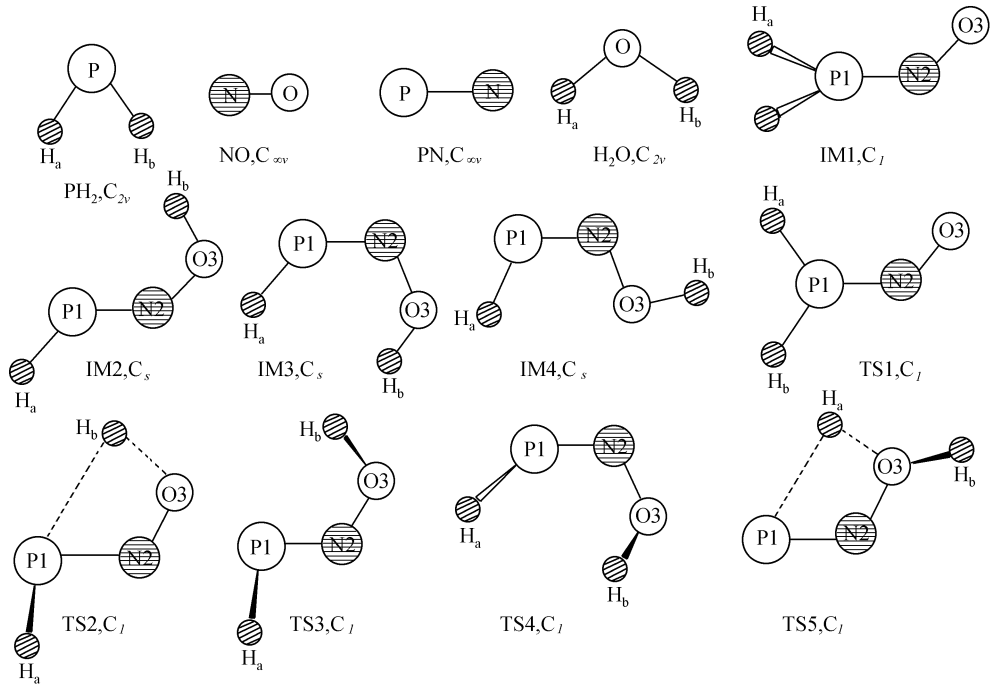

Fig. 1. Schematic diagrams of the reactants, intermediate species, TSs and products, and the optimized geometries at B3LYP/6-31G*.

Table 1 Optimized geometries of reactants, products and intermediate species

Species	Bond length/Å	HF	MP2 (full)	B3LYP	Bond angle(°)	HF	MP2 (full)	B3LYP
$PH_2(C_{2v})$	PH	1.4071	1.4186	1.4304	H_aPH_b	93.5	92.6	91.6
$NO(C_{\infty v})$	NO	1.1270	1.1427	1.1587				
IM1(C_1)	P1N2	1.8096	1.8366	1.9074	P1N2O3	114.9	113.5	114.99
[H_2PNO]	N2O3	1.1768	1.2347	1.1985	H_aP1N2	98.2	97.5	96.6
	H_aP1	1.3996	1.4143	1.4219	H_bP1N2	94.5	93.6	91.95
	H_bP1	1.3979	1.4123	1.4200	D(H_a—O3)	–38.5	–41.1	–40.5
					D(H_b—O3)	–136.4	–138.5	–136.4
IM2(C_s)	P1N2	1.5826	1.6427	1.6333	P1N2O3	119.7	116.4	117.8
	N2O3	1.3373	1.3768	1.3591	H_aP1N2	95.9	93.3	93.8
	H_aP1	1.4004	1.4145	1.4248	$N2O3H_b$	111.4	110.2	110.9
	$O3H_b$	0.9557	0.9881	0.9864	D(H_a—O3)	180	180	180
					D(H_b—P1)	0	0	0
IM3(C_s)	P1N2	1.5700	1.6244	1.6145	P1N2O3	125.4	122.3	123.8
	N2O3	1.3308	1.3670	1.3503	H_aP1N2	100.3	99.3	99.0
	H_aP1	1.4291	1.4481	1.4615	$N2O3H_b$	110.3	108.7	109.3
	$O3H_b$	0.9559	0.9898	0.9877	D(H_a—O3)	0	0	0
					D(H_b—P1)	0	0	0
IM4(C_s)	P1N2	1.5706	1.6291	1.6162	P1N2O3	119.0	115.2	117.5
	N2O3	1.3485	1.3939	1.3767	H_aP1N2	101.2	99.9	100.4
	H_aP1	1.4155	1.4319	1.4447	$N2O3H_b$	104.9	102.4	103.3
	$O3H_b$	0.9489	0.9769	0.9742	D(H_a—O3)	0	0	0
					D(H_b—P1)	180	180	180
$PN(C_{\infty v})$	PN	1.4552	1.5358	1.4946				
$H_2O(C_{2v})$	HO	0.9473	0.9686	0.9686	H_aOH_b	105.5	104.0	103.6

are plane structure except IM1, and TS1 is the only plane structure in the five transition states. The changes in some bond lengths or angles of the five transition states represent the trend of reaction.

Table 2 Optimized geometries of transition states

Species	Bond length/Å	HF	MP2 (full)	B3LYP	Bond angle (°)	HF	MP2 (full)	B3LYP
TS1(C_1)	P1N2	1.7129	1.7189	1.8132	P1N2O3	118.96	125.5	128.9
	N2O3	1.1832	1.2348	1.1848	H_aP1N2	124.3	140.3	153.9
	H_aP1	1.3793	1.4128	1.4398	H_bP1N2	113.8	106.3	98.7
	H_bP1	1.3716	1.3876	1.3896	D(H_a—O3)	0	0	0
					D(H_b—O3)	180	180	180
TS2(C_1)	P1N2	1.7620	1.6763	1.7077	P1N2O3	103.6	102.6	102.9
	N2O3	1.2170	1.3071	1.2745	H_aP1N2	61.4	70.8	68.5
	H_aP1	1.7746	1.6669	1.7137	H_bP1N2	97.8	104.8	103.5
	H_bP1	1.4025	1.4201	1.4283	D(H_a—O3)	6.0	7.2	7.4
					D(H_b—O3)	126.8	139.1	136.8
TS3(C_1)	P1N2	1.5722	1.6360	1.6183	P1N2O3	114.1	109.8	110.9
	N2O3	1.3903	1.4481	1.4370	H_aP1N2	96.0	93.1	93.8
	H_aP1	1.4038	1.4202	1.4317	N2O3H_b	107.9	104.8	105.5
	O3H_b	0.9503	0.9771	0.9738	D(H_a—O3)	178.6	179.1	178.7
					D(H_b—P1)	71.4	74.4	78.8
TS4(C_1)	P1N2	1.5635	1.6240	1.6063	P1N2O3	120.1	116.5	118.3
	N2O3	1.3829	1.4384	1.4249	H_aP1N2	102.3	101.2	101.6
	H_aP1	1.4198	1.4353	1.4488	N2O3H_b	107.2	104.3	105.1
	O3H_b	0.9509	0.9773	0.9740	D(H_a—O3)	–3.4	–3.1	–3.5
					D(H_b—P1)	75.5	77.96	81.7
TS5(C_1)	P1N2	1.5813	1.5885	1.5998	P1N2O3	101.1	99.7	99.4
	N2O3	1.5218	1.6960	1.6680	H_aP1N2	68.3	71.0	70.9
	H_aP1	1.7737	1.7597	1.7464	N2O3H_b	108.2	102.6	105.1
	H_aO3	1.2308	1.3042	1.3029	D(H_a—O3)	–2.6	–2.4	–2.99
	O3H_b	0.9583	0.9899	0.9826	D(H_b—P1)	121.4	111.6	115.9

2.2 Harmonic frequency

In table 3 the harmonic vibrational frequencies of all stationary points were worked out at B3LYP/6-31G* theoretical level, and corrected by scaling a factor 0.9613[25]. Each TS has only one imaginary frequency and is proved to be the first order saddle point on the potential surface, and to be real transition state. From analyzing the vibrational character of imaginary vibration of each transition state, the total effect of vibration of all bonds showed a strong trend of reaction. For example, for TS2 and TS5, the total imaginary vibrational effect of the former responded to H_b atom in PH_2 which departed from P atom, with the bond angle ∠HPN decreased, the joint of H_b with O occurred eventually. While that of the latter responded to the extension of bond NO, and H_a atom escaped from PH_2 to O, so H_2O was formed. Furthermore, the theoretical frequencies were in good agreement with the experimental ones available[26] for both the reactants and products.

2.3 Total energy and relative energy

Total energies of all species were calculated at HF, MP2 and B3LYP with the moderate basis

set 6-31G*. G3 method was applied to all except for transition states. In this paper, total energies, relative energies and ZPEs of all species were applied to analyze the reaction character (table 4). The change trends of relative energies of all species were in excellent agreement.

Table 3 Harmonic frequency (unit: cm^{-1})

Species	Harmonic frequency[a)]	Experimental value[b)]
PH_2	1109.6, 2279.1, 2290. 7	1101.91 (1103), 2310 ± 2
NO	1914.0	1904.04_0 (1904.02_4)
IM1	168.9, 307.0, 444.6, 690.0, 814.0, 1080.8, 1601.2, 2316.5, 2344.4	
IM2	391.8, 511.2, 612.2, 852.1, 929.7, 1082.6, 1389.9, 2303.7, 3322.8	
IM3	416.7, 584.9, 630.4, 803.7, 944.3, 1128.2, 1389.9, 2075.0, 3308.5	
IM4	383.1, 495.6, 612.5, 808.1, 940.1, 1045.8, 1396.6, 2180.8, 3545.9	
TS1	514.2*i*, 267.9, 425.5, 534.2, 645.5, 1027.8, 1639.4, 2171.8, 2483.7	
TS2	1679.7*i*, 420.5, 609.6, 680.8, 836.1, 968.6, 1241.6, 1589.1, 2287.3	
TS3	535.8*i*, 358.1, 608.9, 802.4, 965.2, 1006.0, 1259.4, 2268.0, 3553.3	
TS4	573.0*i*, 380.3, 590.9, 778.9, 926.1, 1028.7, 1260.6, 2154.8, 3552.8	
TS5	1759.9*i*, 441.0, 487.9, 538.0, 908.8, 985.7, 1140.4, 1413.5, 3473.7	
PN	1328.6	1337.24
H_2O	1646.7, 3585.6, 3702.7	1594.59, 3656.65, 3755.79

a) At B3LYP/6-31G* and scaled by 0.9613; b) from ref. [24]

Table 4 Total energy and relative energy (the same 6-31G* basis set)

Species	E/Hf [a)]	E/MP2 [a)]	E/G3 [a)]	E/B3LYP[b)]	ZPE [b)]	ΔE_{rel}[c)]
PH_2+NO	–471.0974824	–471.5102529	–472.178435	–472.3747275	0.017995	0
IM1	–471.0798917	–471.5165467	–472.207594	–472.4002859	0.023148	–67.10
IM2	–471.0736179	–471.5512198	–472.219550	–472.4007780	0.026934	–68.40
IM3	–471.0746167	–471.5514301	–472.220857	–472.4024686	0.026736	–72.83
IM4	–471.0820759	–471.5577262	–472.225677	–472.4069317	0.027036	–84.55
TS1	–471.0257466	–471.5023730		–472.3723387	0.021793	6.27
TS2	–470.9768695	–471.4720356		–472.3353841	0.020461	103.30
TS3	–471.0661508	–471.5423293		–472.3901968	0.025645	–40.61
TS4	–471.0650710	–471.5395188		–472.3891148	0.025294	–37.77
TS5	–470.9792871	–471.4605303		–472.3357014	0.022251	102.46
PN+H_2O	–471.1364964	–471.6294550	–472.287989	–472.4469416	0.024324	–189.60

a) Unit: (×2.6255E3) kJ/mol; b) ZPE corrected by 0.9804, unit: (×2.6255E3) kJ/mol; c) by B3LYP method, unit: kJ/mol.

2.4 Reaction mechanism

Fig. 2 displays the potential energy surface profile for the most favorable reaction channel

$$PH_2+NO \rightarrow PN+H_2O. \quad (1)$$

As the channel is the strongly exothermic reaction, the formation of PN and H_2O[27] can presumably take place among all possible channels. Similar to the reaction NH_2+NO, the channel of the largest exothermic reaction is to form N_2+H_2O and give heat of 523 kJ/mol out. But there is no activation energy barrier in the first addition process of the reaction NH_2+NO[27,28], while from the theoretical result for the reaction PH_2+NO, the first addition reaction must overcome a low activation energy barrier (6.27 kJ/mol) due to the centrifugal barrier resulting from the relative motion of the reactants[29].

Atomic spin density of P in PH_2 is 1.0702 and N in NO is 0.6993, while Mulliken electronic

population of P and N is −0.0059 and 0.1119 (a. u.), respectively. So the addition reaction is an electrophilic reaction due to the strong interaction between P and N atoms. IM1 (H_2PNO) is formed firstly during reaction through a low energy barrier. Successively IM1 rich in energy encounters the first high energy barrier TS2 (four-membered ring structure, 103.3 kJ/mol), the main barrier to the reaction. When it is overcome, 1,3 H-shifting in IM1 occurs to form *trans-cis* isomer IM2 (HPNOH). When the high excited vibrational state PH_2 participates in the reaction, the excited state intermediate will overcome TS2 effectively to facilitate occurrence of the reaction. Xuan and Baugh[1,3] have demonstrated that rate constant of removing $PH_2(v''=1)$ was 100 plus times higher than that of removing ground state PH_2. It is reasonable to believe this phenomenon results from the existence of TS2.

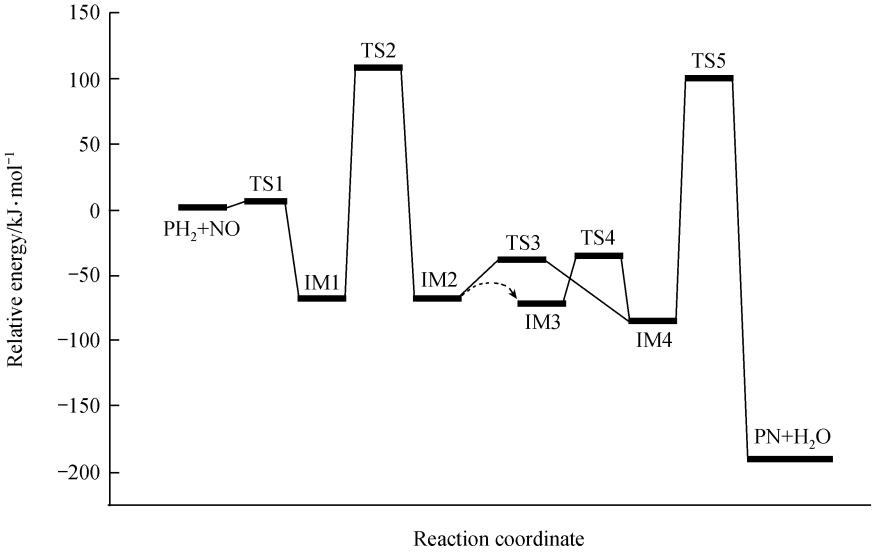

Fig. 2. Schematic diagram of the relative energies of all species.

Isomerization reaction goes on after the formation of IM2. Two paths occur. One is to pass through TS3, a lower energy barrier to form *cis-trans* IM4 by two H atoms rotating around the atom group PNO. The other way is to form IM3, but now we do not know if there is energy barrier existing in this procedure. IM3 will still be isomerized along the favorable direction of reaction till to turn TS4 over. The rotation of H atoms is perpendicular to the molecular plane. The stable isomer IM4 is formed eventually.

Without sudden change on the potential surface during the above procedure, dissociation of intermediate IM4 into products of PN and H_2O encounters an ever higher energy barrier TS5 (102.6 kJ/mol), analogy to TS2, which has the same four-element-ring structure and lies only 0.7 kJ/mol lower than TS2. Based on the structure of IM4, gradually H_a atom (centered on P atom) shifts to O atom and the bond extends till the formation of products, by overcoming the TS5. The

reaction exhausts 189.6 kJ/mol heat.

3 Conclusions

The quantum chemistry computation was performed to the reaction system of PH_2+NO by using molecular orbital *ab initio* and density function theory. The theoretical results indicated that the addition reaction occurred through a low energy barrier TS1 firstly to form IM1, then IM1 was going to isomerize and H atom shifted by rotation to form *trans-cis* IM2. Then the highest barrier TS2, four-element-ring structure with 103.3 kJ/mol, would be turned over, IM2 kept on isomerizing into the forward direction of the reaction. Two H atoms at the edge of IM2 rotated around the molecular plane (PNO) till the formation of *cis-trans* IM4 by two reaction paths. TS5, the sub-high energy barrier 102.6 kJ/mol, was a bridge linking the products and IM4. Also optimized structures and harmonic frequencies of all stationary points were obtained during the theoretical calculation, and the total exothermic was 189.6 kJ/mol.

The formation of PN and H_2O is the most possible reaction channel, and the products are harmless matter. This research may provide us with a potential way for efficient reduction of NO_x pollutants in atmosphere[28].

Acknowledgements This work was supported by the National Natural Science Foundation of China (Grant No. 29773044).

References

1. Xuan, C. N., Margani, A., Reaction of PH_2 ($\tilde{X}^2B_1; v''=0,1$) with NO, Chem. Phys. Lett., 2000, 321: 328—332.
2. Turner, B. E., Tsuji, T., Bally, J. et al., Phosphorus in the dense interstellar medium, Astrophys. J., 1990, 365: 569—585.
3. Baugh, D., Koplitz, B., Xu, Z. et al., PH2 internal energy distribution produced by 193 nm photodissociation of PH3, J. Chem. Phys., 1988, 88: 879—887.
4. Yin, P., Wang, Z. L., Bai, Z. P. et al., A theoretical study on reactivity of singlet phosphinidene by its reacting with polar water molecule, Chem. Phys., 2001, 264: 1—8.
5. Miotto, R., Srivastava, G. P., Ferraz, A. C., Dissociative adsorption of PH3 on Si(100) surface—art. No. 125321, Phys. Rev. B, 2001, 63(12): 5321—5327.
6. Arney, D., Schnabel, R. C., Scott, B. C. et al., Preparation of actinide phosphinidene complexes: Steric control of reactivity, J. Am. Chem. Soc., 1996, 118: 6780—6781.
7. Courtin, R., Gautier, D., Marten, A. et al., Composition of Saturn's atmosphere at northern temperate latitudes from Voyager iris spectra: NH_3, PH_3, C_2H_2, C_2H_6, CH_3D, CH_4, and the saturnian D/H isotopic ratio, Astrophys. J., 1984, 287: 899—916.
8. Tokunaga, A. T., Knacke, R. F., Ridgway, S. T. et al., High-resolution spectra of Jupiter in the 744—980 inverse centimeter spectral range, Astrophys. J., 1979, 232: 603—615.
9. Noll, K. S., Larson, H. P., The spectrum of Saturn from 1990 to 2230/cm——Abundances of AsH3, CH3D, CO, GeH4, NH3, and PH3, Icarus (International Journal of the Solar System), 1991, 89: 168—189.
10. Stringfllow, G. B., Organomtallic Vapor-Phase Epitaxy: Theory and Practice, New York: Academic Press, 1989.
11. Manasevit, H. M., Hewitt, W. B., Nelson, A. J. et al., The use of metalorganics in the preparation of semiconductor materials, J. Electrochem. Soc., 1989, 136: 3070.
12. Pierini, A. B., Duca, Jr. J. S., Semiempirical evaluation for proton affinities of phosphorus compounds, Int. J. Quant. Chem., 1993, 48: 343—354.
13. Jursic, B. S., Complete basis set, the MP2 *ab initio*, and hybrid density functional theory valuation of ionization potential

and electron affinity for PH, PH_2, PHF, PF, and PF_2, J. Mol. Struct. (Theochem), 2000, 507: 11—16.

14. Woodcock, H. L., Wesolowski, S. S., Yamaguchi, Y. et al., A systematic study of the $\tilde{X}^2B_1$ $\tilde{A}^2A_1$, and $\tilde{B}^2B_2$ states of the neutral radical PH_2, J. Phys. Chem. A, 2001, 105: 5037—5045.
15. Goto, M., Saito, S., Submillimeter-wave spectra of PH and PD radicals, Chem. Phys. Lett., 1993, 211: 443—448.
16. Mercier, F., Deschamps, B., Mathey, F., Terminal aminophosinidene complex, a new approach, J. Am. Chem. Soc., 1989, 111: 9098—9100.
17. El-Nahas, A. M., Hirao, K., Complexation of Li^+ and Cu^+ with HX (X = F, Cl, OH, SH, NH_2, and PH_2) molecules by B3LYP and CCSD(T) methods, J. Phys. Chem. A, 2000, 104: 138—144.
18. Wang Mingxing, Atmospheric Chemistry (in Chinese), 2nd ed., Beijing: Meteorological Press, 1999, 360—366.
19. Wang Zhenya, Li Haiyang, Zhou Shikang, Research progress on ozone depletion chemistry in stratosphere, Chinese Science Bulletin, 2001, 46(8): 619—625.
20. Xuan, C. N., Margani, A., Collision induced deactivation of PH_2 ($\tilde{A}^2A_1$:v_2'=1, 0) and PH_2($\tilde{X}^2B_1$:v_2'=1) by diatomic molecules, J. Chem. Phys., 1998, 109: 9417—9424.
21. Hu Zhengfa, Wang Zhenya, Kong Xianglei et al., Photoionization and photodissociation mass spectroscopy of methylamine by synchrotron radiation, Acta Physica Sinica (in Chinese), 2002, 51(2): 235—239.
22. Frisch, M. J., Trucks, G. W., Schlegel, H. B. et al., Gaussian 98, Revision A.7, Pittsburgh PA: Gaussian, Inc., 1998.
23. Wang Zunyao, Xiao Jijun, Ji Guangfu et al., Mechanism and application of reaction Cl_2+2HBr=2HCl+Br_2, Science in China (in Chinese), Ser. B, 2001, 31(3): 205—213.
24. Herzberg, G., Molecular Spectra and Molecular Structure, Vol. 1, Spectra of Diatomic Molecules, 2nd ed., New York: Van Nostrand, 1979, 558—559.
25. Foresman, J. B., Frisch, M. J., Exploring Chemistry With Electronic Structure Methods, 2nd ed., Pittsburgh PA: Gaussian Inc., 1998, 64—65.
26. Jacox, M. E., Ground-state vibrational energy levels of polyatomic transient molecules, J. Phys. Chem. Ref. Data, 1998, 27: 945—1180.
27. Phillips, L. F., A priori rate constant for the reaction NH_2+NO, Chem. Phys. Lett., 1987, 135: 269—274.
28. Heal, M. R., Pilling, M., The Chemical Dynamics and Kinetics of Small Radicals (1) (eds. Liu, K. P., Wagner, A.), Singapore: World Scientific, 1995, 3—38.
29. Langford, A. O., Moore, C. B., Reaction and relaxation of vibrationally excited formyl radical, J. Chem. Phys., 1984, 80: 4204—4210.